Duan *et al. Biochar* (2025) 7:78
https://doi.org/10.1007/s42773-025-00475-x

Biochar

ORIGINAL RESEARCH Open Access

Modulating biochar compositions to maximize synergy between contaminant binding and transformation: the critical role of carbonates and implications for in situ groundwater remediation

Lin Duan[1], Zicui Gong[1], Yang Li[1], Tianchi Cao[1], Tong Zhang[1*] and Wei Chen[1*]

Abstract

Dealing with groundwater impacted by persistent, low-concentration chlorinated solvents is a major challenge for site remediation, as technologies designed for fast contaminant removal or destruction often are not cost-effective. For long-term plume management, in situ contaminant sequestration using carbonaceous materials is a more viable strategy. Here, we prove the concept that the effectiveness of this approach can be improved by modulating the compositional and surface properties of carbonaceous materials to maximize the synergy between contaminant binding and abiotic transformation. We found that two pine wood biochars pyrolyzed at 600 and 700 °C exhibit not only faster adsorption kinetics for 1,1,2,2-tetrachloroethane than those prepared at lower temperatures (500 °C and below), but also greater efficacy in enhancing the dehydrochlorination of the contaminant. The higher catalytic efficiency is counterintuitive, as it is commonly accepted that surface carboxyl and phenolic groups are the catalytic sites. With supplementary experiments carried out using modified materials and at varied pH values, we found that the surprisingly higher catalytic activities of these two samples are due to their higher carbonate contents. Interestingly, trichloroethylene, the hydrolysis product, is more adsorptive to the biochars than the parent compound. Thus, by promoting the abiotic transformation, these two biochars enable much more effective plume interception than the less-reactive materials. The findings have important implications for dealing with long-term, persistent groundwater contamination, particularly, the "rebounding" problem often occurring post active site remediation.

Highlights

- High-temperature biochars were more effective in catalyzing hydrolysis of TeCA.
- Carbonates were primary nucleophiles catalyzing hydrolysis of surface-bound TeCA.
- Biochar-mediated transformation of TeCA improved contaminant sequestration.

Keywords Biochar, Chlorinated solvents, Hydrolysis, Permeable reactive barrier, Groundwater remediation

*Correspondence:
Tong Zhang
zhangtong@nankai.edu.cn
Wei Chen
chenwei@nankai.edu.cn
Full list of author information is available at the end of the article

Graphical Abstract

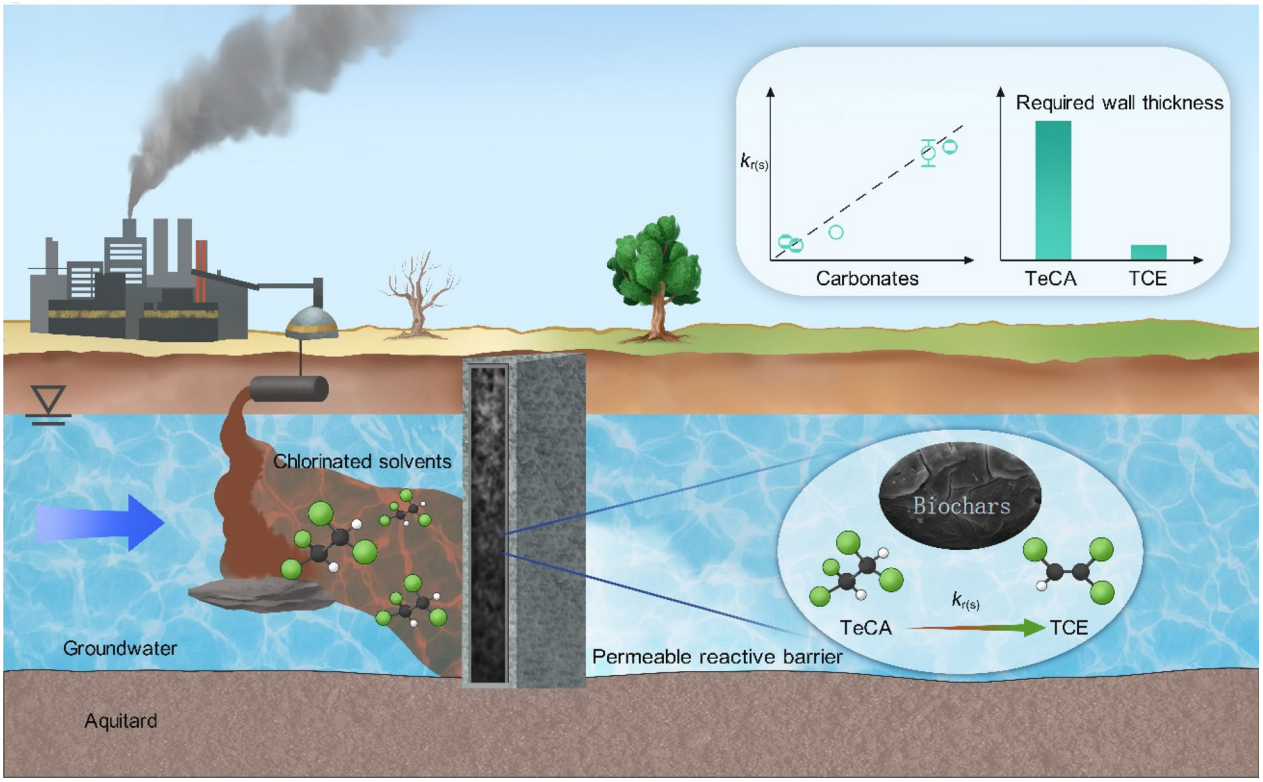

1 Introduction

Groundwater contamination is a worldwide environmental problem, posing serious risks to the ecosystems and human health (Li et al. 2024; Moran et al. 2007; Zhang et al. 2017). Dealing with groundwater impacted by chlorinated solvents, which often persist in subsurface for prolonged periods of time, is particularly challenging (Hou et al. 2023; Stroo and Ward 2010). Currently, there are numerous sites contaminated with chlorinated solvents, including over 50% of the US Environmental Protection Agency's Superfund sites (Hou et al. 2023; Liang et al. 2024; Moran et al. 2007). Various technologies have been developed for the cleanup of chlorinated solvent-impacted sites. Some of the commonly adopted ones include in situ thermal desorption, in situ chemical oxidation or reduction, air stripping, soil vapor extraction, cosolvent and surfactant flushing, and enhanced biodegradation (Ellis and Hadley 2009; Stroo and Ward 2010). Many of these approaches are effective for fast removal or destruction of large mass of contaminants, but are less cost-effective when dealing with persistent, low-concentration contamination, a common situation at the later stage of remediation (e.g., after the bulk of the contaminants is removed with aggressive approaches such as thermal desorption or chemical oxidation) (ITRC 2011; Nivorlis et al. 2024; USEPA 2008). To avoid excessive reagent consumption and high costs of field deployment, it is critical to develop cost-effective technologies for long-term plume management.

One strategy to deal with groundwater contamination by persistent, low-concentration chlorinated solvents is using carbonaceous materials to sequester contaminants and intercept contaminant plume. Owing to their high surface areas, strong hydrophobicity, and porous structures, carbonaceous materials are effective adsorbents for many chlorinated compounds (Mauter and Elimelech 2008; Pavlostathis and Jaglal 1991; Pignatello et al. 2017; Zhou et al. 2015). For example, it was reported that the adsorption coefficient of trichloroethylene (TCE)—a common chlorinated compound in groundwater—to granular activated carbon can reach up to 17,000 L kg^{-1} (Zhou et al. 2015), over four orders of magnitude larger than the values reported for mineral oxides (0.3–0.4 L kg^{-1}) and soils (0.1–12 L kg^{-1}) (Pavlostathis and Jaglal 1991). For in situ remediation, these materials may be placed in a permeable reactive barrier (PRB) as fillings

(Stroo and Ward 2010; Zhang et al. 2017), or injected into the contaminated sites in the form of colloidal suspensions (Fan et al. 2017; Simon 2015). Both have been shown to be effective in preventing contaminant migration. The commonly used carbonaceous materials for these purposes are activated carbons, whereas biochars and carbonaceous nanomaterials (e.g., graphene oxides and carbon nanotubes) have also been researched (Chen et al. 2008, 2015; Jiang et al. 2023; Lu et al. 2020; Qiu et al. 2022; Shen et al. 2015; Sizmur et al. 2017; Twagirayezu et al. 2024; Zhu et al. 2022).

Besides of serving as adsorbents, carbonaceous materials may also mediate abiotic or biotic degradation (Cao et al. 2024; Chen et al. 2014a, b, 2023; Ding et al. 2018; Hsieh and Pignatello 2017; Khalili et al. 2024; Li et al. 2022; Mackenzie et al. 2005; Pignatello et al. 2017; Seenthia et al. 2024; Xie et al. 2023; Xu et al. 2020; Yang et al. 2022, 2016; Yuan et al. 2017). For example, carbonaceous materials may serve as electron shuttles to enhance anaerobic dehalogenation of chlorinated solvents (Chen et al. 2023; Yuan et al. 2017), or enhance hydrolysis reactions by providing acidic/basic sites (Chen et al. 2014a, b; Hsieh and Pignatello 2017). Thus, by carefully designing the surface properties of a carbonaceous material, one can maximize the performance of these materials through combined contaminant sequestration and transformation. For instance, by converting a less adsorptive compound to a more adsorptive one, or turning a less biodegradable compound into one with higher microbial degradation potential, the efficacy in plume management can be greatly enhanced.

Here, It showed that tuning chemical compositions of biochars to enhance their capabilities in catalyzing the hydrolysis reactions of chlorinated solvents significantly enhances the performance of these materials. Specifically, two pine-wood biochars pyrolyzed at 600 and 700 °C are more effective in promoting dehydrochlorination of 1,1,2,2-tetrachloroethane (TeCA), a common chlorinate solvent in groundwater, than three biochars prepared at lower temperatures (300, 400 and 500 °C). Fitting the reaction kinetic data using a multi-step model indicates that the hydrolysis rate constants of TeCA on the surface of the two high-temperature biochars are 2.6–3.0 times higher than that observed in homogeneous aqueous solution. With supplementary experiments carried out using surface modified materials and at varied pH, we found that carbonates are the primary nucleophiles catalyzing the reaction. Notably, the high-temperature biochars exhibit much higher adsorption affinity for TCE, the hydrolysis product, than for the parent product TeCA. Modeling results showed that when using these materials as the fillings of PRB, the wall thickness can be greatly shortened. Findings of this research have important implications for dealing with long-term, persistent groundwater contamination, particularly, for preventing "rebound" that commonly occurs post active site remediation.

2 Materials and methods

2.1 Chemicals and reagents

TeCA (above 99%) and TCE (above 99%) were purchased from Sigma Aldrich (St. Louis, MO, USA). The physicochemical properties of TeCA and TCE are presented in Additional file 1: Table S1. All organic solvents used were of chromatography grade and other chemicals used were of reagent grade.

2.2 Preparation and characterization of biochar samples

Pine wood was selected as the feedstock for biochar production. Prior to pyrolysis, the pine wood was thoroughly washed with deionized water, then oven-heated at 60 °C overnight, and subsequently ball-milled to achieve a uniform size. The dried material was then transferred into a furnace and subjected to pyrolysis under a continuous nitrogen flow. The temperature was gradually increased at a rate of 5 °C min^{-1} until the desired target temperature (300, 400, 500, 600 and 700 °C) was reached, where it was held for 4 h. After pyrolysis, the samples were cooled to room temperature, then sieved through a 60-mesh sieve and stored in a desiccator for subsequent use (Chen et al. 2015; Fang et al. 2014). The resulting samples were labeled as BC300, BC400, BC500, BC600, and BC700, corresponding to the respective pyrolysis temperatures. Additionally, approximately 1 g of BC300 or BC700 was subjected to acid treatment by immersion in 50 mL of 0.05 mM hydrochloric acid for 12 h to obtain "acid-treated biochars". After the acid treatment, the samples were thoroughly washed with deionized water until pH stabilized, then dried at 105 °C overnight (Chen et al. 2008; Xiao et al. 2020). The acid-treated biochar samples were referred to as ATBC300 and ATBC700.

The morphology and physical dimensions of the biochar samples were examined using scanning electron microscopy (SEM) (Nova Nano SEM 230, Hillsboro, USA). Fourier-transform infrared (FTIR) analysis was performed using a Bruker TENSOR 27 apparatus (Bruker Optics Inc., Germany). The elemental composition was determined using a Vario EL cube CHO element analyzer (Elementar, Germany). The surface organic alkalinity of biochar materials, including carboxyl groups (RCOOH) and phenolic hydroxyl groups (ROH), was quantified using the Boehm titration method. These groups contributed to alkalinity when deprotonated (Fidel et al. 2013, 2017). Inorganic alkaline species, including carbonates and other inorganic alkalis, were quantified and calculated according to previously reported methods (Fidel

et al. 2017). Detailed information is presented in Additional file 1: Text S1.

2.3 Hydrolysis reaction of TeCA in homogeneous solution and in biochar suspension

Reaction kinetic experiments were conducted in aqueous solution both in the absence and presence of biochar samples. Approximately 40 mL of an electrolyte (containing 0.05 M K_2HPO_4/KH_2PO_4 as the pH buffer) was added to each 40 mL amber glass vial. The pH of the solution was adjusted to 7, 8, or 9 with HNO_3 or NaOH. The pH values and ionic strength were selected to represent typical solution chemistry conditions in groundwater (Hao et al. 2025; Qureshi et al. 2021). For the experiment involving biochars, 0.1 g biochar was added to the vial before adding the electrolyte solution, and the mixture was placed on an orbital shaker (7 rpm) for 24 h. Then, a TeCA stock solution (in methanol) was injected into the solution with a micro-syringe, to give an initial TeCA concentration of 5 mg L^{-1}; this concentration was selected based on the field studies previously reported (Bekele et al. 2019; Wilkin et al. 2019). Next, the vial was full-filled with buffer solution, sealed immediately, and left on an orbital shaker (7 rpm) operated at 25 °C. At the predetermined time intervals, 1.0 mL of the supernatant was withdrawn, and transferred to a clean glass vial containing a pH 3 buffer solution (0.05 mol L^{-1} KH_2PO_4, pH adjusted with HNO_3) to terminate the reaction. The solution was filtrated through a 0.22-μm membrane filter and then extracted with *n*-hexane. The hexane extract was then analyzed to determine the concentrations of TeCA and TCE. The pH values of the solution were monitored during the sampling and were found to be essentially unchanged in all the experiments.

For the extraction of biochar-bound TeCA and TCE, a method modified from the EPA Method 3550c (Chen et al. 2014a) was used. Each sample was transferred to a 20 mL glass vial, and 16 mL of acetone was added. The mixture was sonicated for 30 min, then centrifuged, and the supernatant was collected. This extraction process was repeated for three times with fresh acetone. The extracts from all three extractions were combined for the determination of the total mass of TeCA and TCE extracted from the biochar. The concentrations of TeCA and TCE in extracts were determined with an Agilent 6890 N gas chromatography with electron capture detector (GC-ECD) (Agilent Technologies, Santa Clara, CA, USA) equipped with an HP-5 capillary column (30 m × 0.32 mm × 0.25 μm).

2.4 Adsorption of TeCA and TCE to biochar

The adsorption of TeCA and TCE onto selected biochar samples was investigated using a batch adsorption method, as described in our previous studies (Chen et al. 2014b). The experiments were conducted in 40-mL amber EPA vials with Teflon-lined screw caps, and maintained at a pH of 3. Detailed experimental procedures are given in the Additional file 1: Text S2. Each adsorption isotherm contained of six individual data points, and each data point were measured in duplicate.

2.5 Modeling of reaction kinetics data

A multistep kinetic model was developed and simulated using MATLAB software (The Mathworks, Inc.). The adsorption and reaction kinetic data were fitted using the Fmincon function. The optimized values were obtained by solving the differential equations using the function ode 45. The reaction rate constants were determined by minimizing the sum of squared error, and the goodness of fit to the model was assessed using an error distribution diagram (Additional file 1: Fig. S1). Besides, the breakthrough of TeCA and TCE from a PRB was simulated at selected simulation time (100 d and 1000 d) using the one-dimensional advection–dispersion equation, which was also modeled in MATLAB software.

3 Results and discussion

3.1 Physicochemical characteristics of the biochar samples

The two biochar samples obtained at the higher temperatures (BC600 and BC700) differed substantially from those obtained at the lower temperatures in terms of morphology, surface O-functionalities, and alkaline components. The SEM images showed that the biochar samples obtained at the lower pyrolysis temperatures (i.e., BC300, BC400, and BC500) were composed of irregular particles with relatively smooth surfaces (Fig. 1a). In contrast, the surfaces of BC600 and BC700 were rough and wrinkled, with visible cracks (Fig. 1a). The FTIR spectra (Fig. 1b) showed the O–C–O, C–O, C=O, and –OH stretching bands (at 1030, 1200, 1700, and 3400 cm^{-1}, respectively) for BC300, whereas these peaks were not observed for BC600 and BC700. The elemental composition analysis further showed that the oxygen contents of the biochar samples decreased with pyrolysis temperature, whereas an opposite trend was observed for the carbon contents (Fig. 1b and Additional file 1: Table S2).

The pyrolysis temperature also affected the compositions of the alkaline species substantially. The relative contents of organic alkalis (i.e., RCOOH and ROH) decreased with pyrolysis temperature—while these were the predominant alkaline species of BC300 and BC400, they only accounted for a small fraction of the total alkalis for BC600 and BC700 (Fig. 1c, Additional file 1: Table S3). For BC600 and BC700, inorganic alkalis were the predominant alkaline species. In particular, carbonates accounted for 55% of the total alkalis for BC600 and

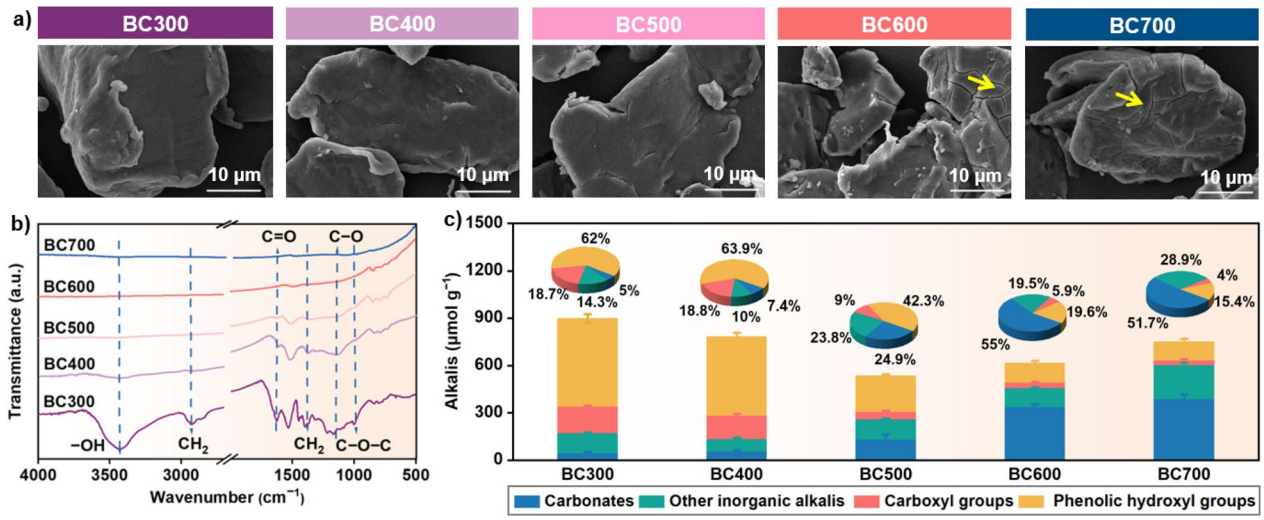

Fig. 1 Characterization of pine wood-derived biochar samples obtained at different pyrolysis temperatures. **a** Scanning electron microscope (SEM) images. The yellow arrows highlight the formation of cracks on the two biochars prepared at higher pyrolysis temperatures (BC600 and BC700). **b** Fourier transform infrared (FTIR) spectra. **c** Contents of different inorganic and organic alkaline species

52% for BC700 (Fig. 1c); for BC300 and BC400, these components only contributed to 5–7% of the total alkalis (Fig. 1c). The amounts of the other inorganic alkalinity (primarily Fe/Al hydroxides (Fidel et al. 2017)) were similar among all five biochar samples (Fig. 1c). Since the hydrolytic reaction of TeCA is base-promoted, the differences in the distribution of alkaline species among these samples indicate that their catalytic efficiencies likely will differ markedly.

3.2 Biochars prepared at higher pyrolysis temperatures are more effective in catalyzing hydrolysis of TeCA

The two biochar samples obtained at 600 and 700 °C markedly enhanced the hydrolysis of TeCA, whereas the three samples prepared at lower pyrolysis temperatures (500 °C or below) inhibited TeCA degradation. The kinetics of both TeCA degradation and TCE formation were faster in the presence of BC600 and BC700, compared with the rates observed for the reaction in homogeneous aqueous solutions (i.e., in the absence of a biochar sample); in contrast, the presence of BC300, BC400 or BC500 resulted in slower degradation kinetics, with the effects more pronounced for BC300 and BC400 (Fig. 2a–d). The extents of TeCA degradation and TCE formation at the end of the experiments followed the order of BC700 > BC600 > aqueous solution > BC 500 > BC400 > BC300.

The detailed kinetic data (Fig. 2e–j) showed that the mass of TeCA adsorbed to the low-temperature biochars (BC300, BC400 and BC500) reached a maximum value in the early stage of the experiments (due to the fast adsorption kinetics) and then changed little with time (Fig. 2f–h), indicating the low reactivity of TeCA adsorbed to these surfaces. For the experiments involving BC600 and BC700, after the mass of the surface-accumulated TeCA peaked, it then decreased readily (Fig. 2i, j). The pie charts further showed that in the experiments of BC600 and BC700, only 11–14% of the initially added TeCA molecules remained after 284 h; for the low-temperature biochars, this was as high as 50–60%. Additionally, in the experiments of BC300 and BC400, a large fraction of TeCA remained in the aqueous solution. The reaction product, TCE, exhibited a high tendency to absorb to the biochars (in all the experiments, the mass of TCE in the aqueous phase was negligible); the mass of adsorbed TCE continuously increased with prolonged reaction time, particularly for BC600 and BC700.

Hydrolysis of TeCA occurred both in the aqueous phase and on biochar (Fig. 3a), and the evolution of TCE mass on the biochars was controlled simultaneously by the degradation of surface-bound TeCA and the adsorption of TCE from the aqueous solution. To quantitatively discern the contribution of surface reaction vs. adsorption, the kinetics data in Fig. 2a were fitted with a multi-step kinetic model (the conceptual model and the differential equations in Fig. 3a; the model fitted curves and parameters are shown in Additional file 1: Fig. S2 and Table S4). Clearly, TeCA molecules adsorbed on the surfaces of BC600 and BC700 underwent faster degradation than those in the aqueous solution, as indicated by the model-fitted $k_{r(s)}$ and $k_{r(aq)}$ values; in contrast, degradation of TeCA adsorbed to BC300, BC400 and BC500 was slower than in homogeneous aqueous solution (Fig. 3b). The inability of these three biochars in enhancing TeCA hydrolysis was unexpected, as previous studies carried

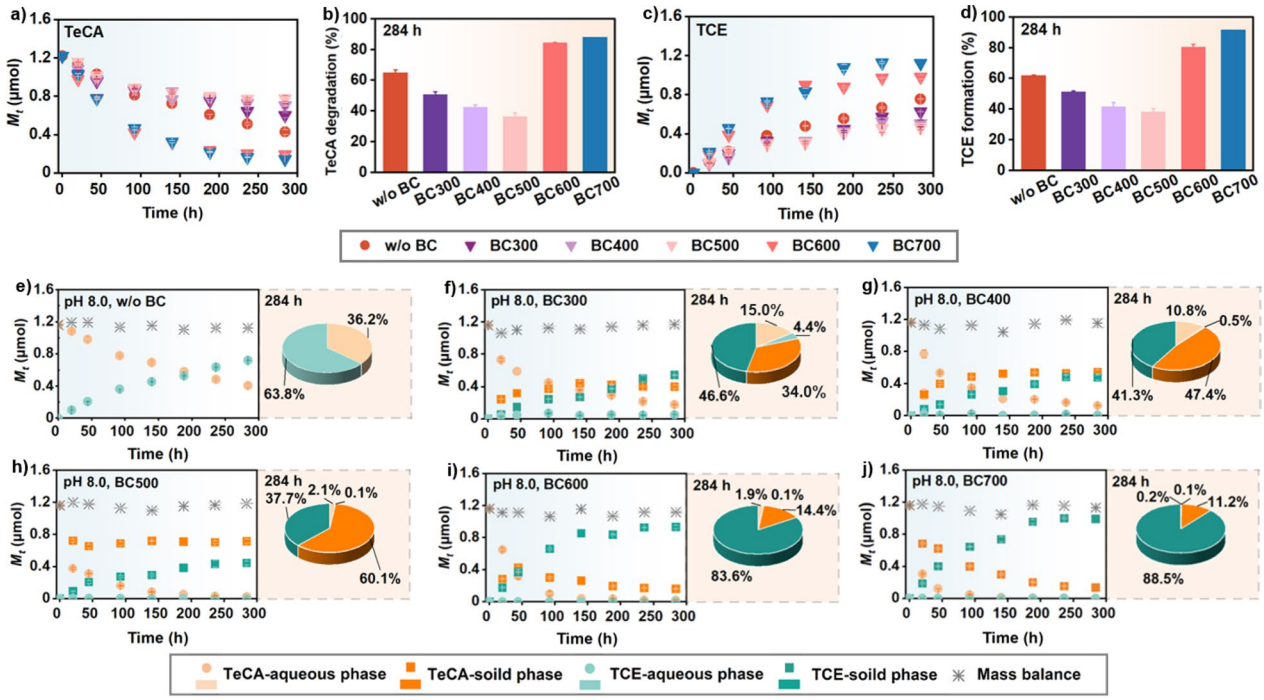

Fig. 2 Biochars prepared at higher pyrolysis temperatures are more effective in catalyzing hydrolysis of TeCA. **a**–**d** Kinetic of TeCA degradation and TCE formation. The histograms show the efficiency TeCA degradation and TCE formation at 284 h. **e**–**j** Changes of the mass of different TeCA and TCE species with time. The pie charts show the mass fractions of TeCA and TCE species at 284 h. Error bars indicate variances of duplicates. The concentration of biochar was 2.5 g L^{-1}, the initial mass of TeCA was 1.2 μmol, solution pH was 8.0 with 0.05 M K_2HPO_4/KH_2PO_4 as the pH buffer, and the reaction was carried out at 25 °C in the dark

out using activated carbon (Chen et al. 2014a), functionalized carbon nanotubes (Chen et al. 2014b), graphene-based nanomaterials (Li et al. 2016), and biochar-derived dissolved organic carbon (Chen et al. 2024) all indicated that the deprotonated RCOOH and ROH groups serve as the bases to promote the β-elimination reaction. Thus, the markedly different kinetics of surface-bound TeCA as observed in this study indicate that other components, rather than O-functional groups, were the primary catalytic sites of the biochars (Notably, the adsorption kinetics of both TeCA and TCE, as indicated by the fitted adsorption rate constants (k_a), increased with the pyrolysis temperature of the biochars (Fig. 3c). Faster adsorption of TeCA to the biochars would facilitate its degradation at surface catalytic sites; however, the small differences in k_a values indicated that this was only a minor cause).

3.3 Carbonates are the primary components catalyzing hydrolysis of surface-bound TeCA

The fact that the biochars obtained using high pyrolysis temperatures enhanced TeCA degradation to much greater extents was attributable to their high carbonate contents. The hydrolysis of TeCA is a base-catalyzed reaction, in that, a nucleophile (e.g., OH^-) attacks the hydrogen atom attached to the β-carbon atom, which facilitates the leaving of the Cl atom from the α-carbon and the formation of a π bond, with TCE being the sole degradation product (Chen et al. 2014b; Mackenzie et al. 2005). Besides of OH^- ions, surface alkaline groups (e.g., deprotonated RCOOH and ROH) have also been shown to act as nucleophiles to promote the reaction (Chen et al. 2014a, b, 2024; Li et al. 2016; Xu et al. 2017). Indeed, the surface reaction constants of TeCA ($k_{r(s)}$) correlated closely with the total concentrations of alkalis of the biochars (R^2 = 0.915) (Fig. 4a). However, a closer examination on the correlation between $k_{r(s)}$ and the contents of individual alkaline species of the biochars revealed that a linear correlation was only observed for carbonates, with an even higher R^2 value (0.967) than that observed for total alkalis (Fig. 4b). In contrast, the correlation between $k_{r(s)}$ and the content of other inorganic alkalis was poor (R^2 = 0.464), so was the correlation with the surface carboxyl groups (Fig. 4c, d). Thus, the linear regression results suggest that carbonates were the predominant constituents of the biochars catalyzing TeCA degradation. Within the pH range of the TeCA hydrolysis experiments, carbonates (i.e., salts of bicarbonate

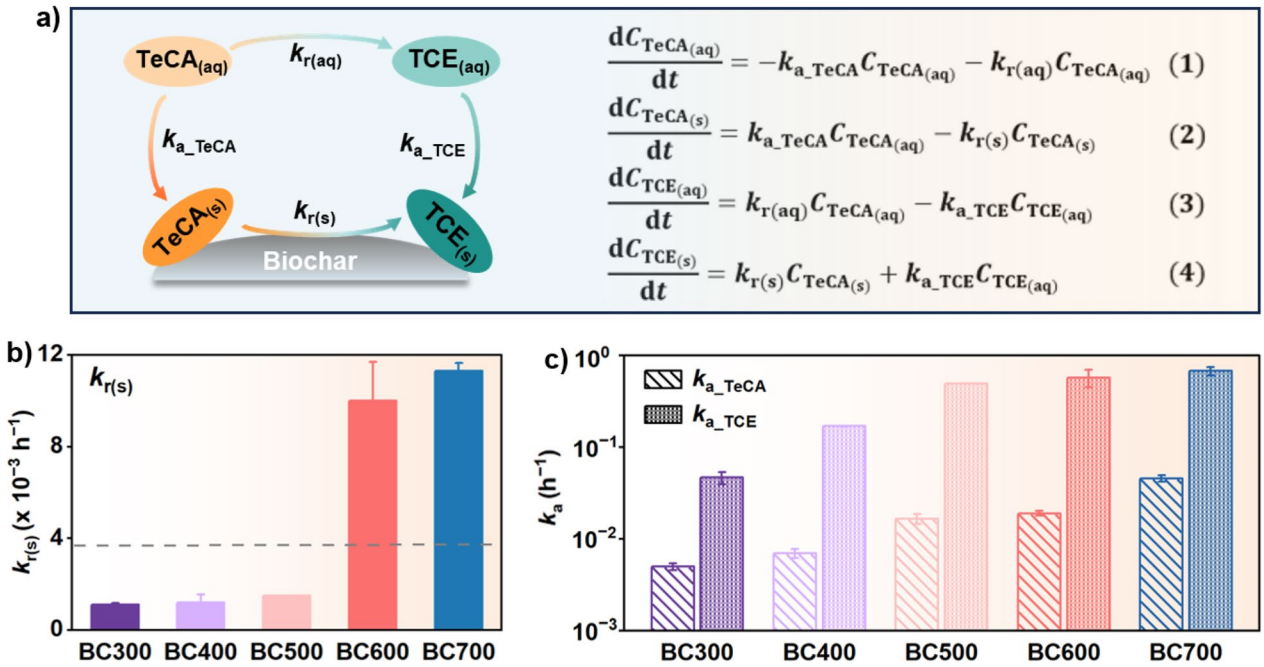

Fig. 3 The higher catalytic efficacies of BC600 and BC700 are mainly due to surface-enhanced TeCA degradation. **a** The reaction scheme and the multi-step kinetic model used to fit the reaction kinetic data. **b** Comparison of model-fitted surface hydrolysis rate constants of TeCA ($k_{r(s)}$) in the presence of different biochars. The dashed line represents the reaction rate constant of TeCA ($k_{r(aq)}$) in homogeneous aqueous solution. **c** Comparison of model-fitted adsorption rate constant of TeCA (k_{a_TeCA}) and TCE (k_{a_TCE}) to different biochars

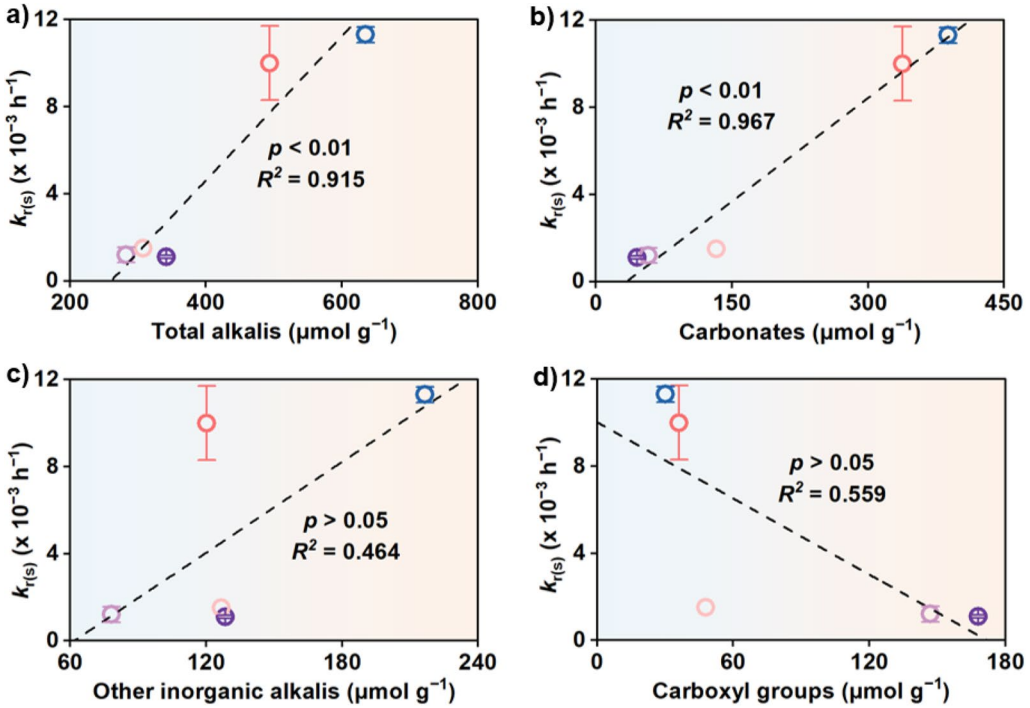

Fig. 4 Carbonates are the primary component catalyzing hydrolytic degradation of adsorbed TeCA. **a**–**d** Correlations between hydrolysis rate constants of adsorbed TeCA at pH 8.0 and the contents of total alkalis, as well as the contents of individual alkaline components including carbonates, other inorganic alkalis, and carboxyl groups

and carbonate) could consume protons and increase the concentrations of the nucleophilic OH^- ions: $CO_3^{2-} + 2H_2O \leftrightarrow H_2CO_3 + 2OH^-$; $HCO_3^- + H_2O \leftrightarrow H_2CO_3 + OH^-$. Moreover, at pH 8 carbonates were mainly in the form of HCO_3^-, a nucleophile nearly as potent as OH^- (Schwarzenbach et al. 2017). The high concentrations of HCO_3^- and OH^- on the surfaces of the biochars would have promoted the transformation of adsorbed TeCA. (Notably, the increase of carbonate contents with biochar pyrolysis temperature was consistent with the literature Fidel et al. 2017; Stratford et al. 2014; Xiao et al. 2018; Yuan et al. 2011)).

To verify that carbonates were the primary catalytic sites for TeCA degradation, supplementary experiments were carried out using biochar samples treated with hydrochloric acid to partially remove the carbonates (Additional file 1: Fig. S3). The $k_{r(s)}$ values of adsorbed TeCA on the acid-treated BC700 (referred to as ATBC700) was over 30% lower than that of TeCA on the pristine BC700 (Fig. 5a). In comparison, the $k_{r(s)}$ values of TeCA adsorbed on the acid-treated BC300 (ATBC300) and on the untreated BC300 were comparable (Fig. 5b). This corroborated the important role of carbonates in catalyzing the reaction – BC700 had a higher carbonate content, thus, removing carbonates through acid treatment substantially compromised its catalytic efficacy; in comparison, the carbonate content of BC300 was low, therefore, the loss of carbonates had a much lower impact on its ability to catalyze the reaction. Moreover, the pH-dependent experiments carried out within a pH range of 7–9 (Additional file 1: Fig. S4) showed that the difference in $k_{r(s)}$ between TeCA on BC700 and on BC300 was substantial at pH 7 and 8, 16 and 6.0 times, respectively (Fig. 5c, d), but was considerably smaller at pH 9 (in this case, the $k_{r(s)}$ value of BC700 was only 1.6 times that of BC300; Fig. 5e). This was consistent with the low carbonate contents of BC300 – the organic alkaline sites on BC300 (e.g., RCOOH and ROH) would only become deprotonated and nucleophilic at relatively higher pH (Chen et al. 2014b).

Notably, metal atoms on the surface of metal oxides may react with water molecules, generating metal-hydroxo species that serve as nucleophiles to catalyze the hydrolysis reactions (Li et al. 2018; Xu et al. 2017). However, the correlation between $k_{r(s)}$ and the content of other inorganic alkalis (primarily Fe/Al hydroxides) was poor (Fig. 4c), indicating these metal oxides played a much lesser role than carbonates in promoting hydrolysis of surface-adsorbed TeCA.

3.4 Biochar-mediated transformation of TeCA significantly improves contaminant sequestration

The transformation of the less adsorptive TeCA to the more adsorptive TCE significantly improves contaminant sequestration by biochars. Taking BC600 as an example, the calculated distribution coefficients (K_d) of TCE are over two orders of magnitude higher than that of TeCA (Fig. 6a; Additional file 1: Table S5). This observation was remarkable, as the two contaminants have similar hydrophobicity and molecular diameters

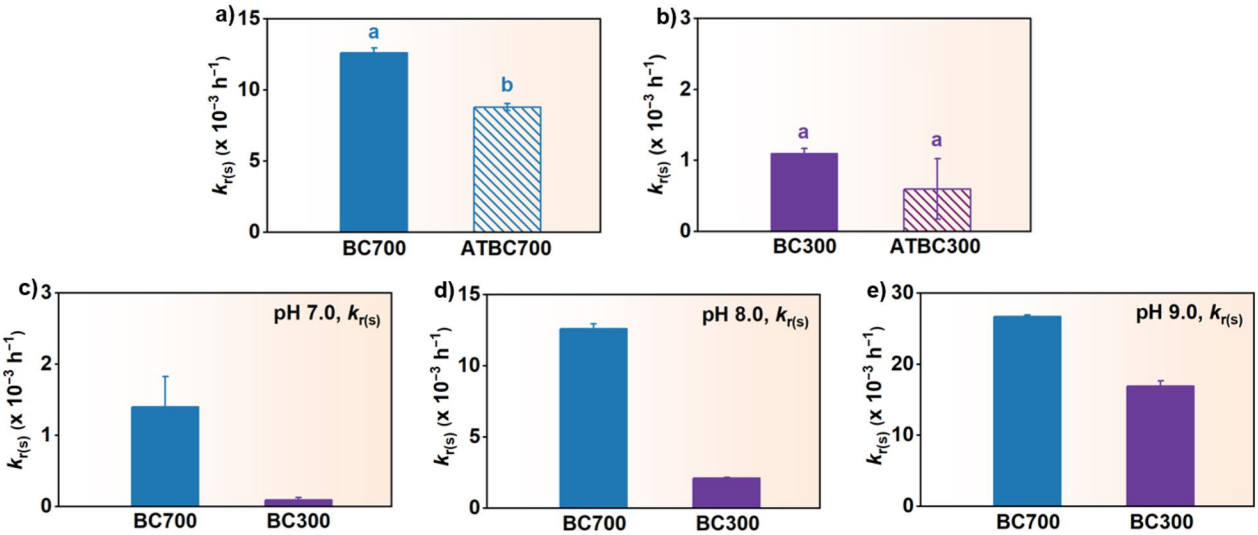

Fig. 5 The high reaction rates of TeCA adsorbed to the high-temperature biochars are in line with the high carbonate contents of the materials. **a**, **b** Comparison of hydrolysis rate constants of TeCA adsorbed on pristine as-prepared biochars (BC300 and BC700) and acid treated biochars (ATBC300 and ATBC700), confirming the catalytic role of carbonates. **c**–**e** Comparison of hydrolysis rate constants of TeCA adsorbed to BC700 vs. BC 300 at different pH values, confirming that the difference is the largest when carbonates are the primary catalytic sites (i.e., at lower pH)

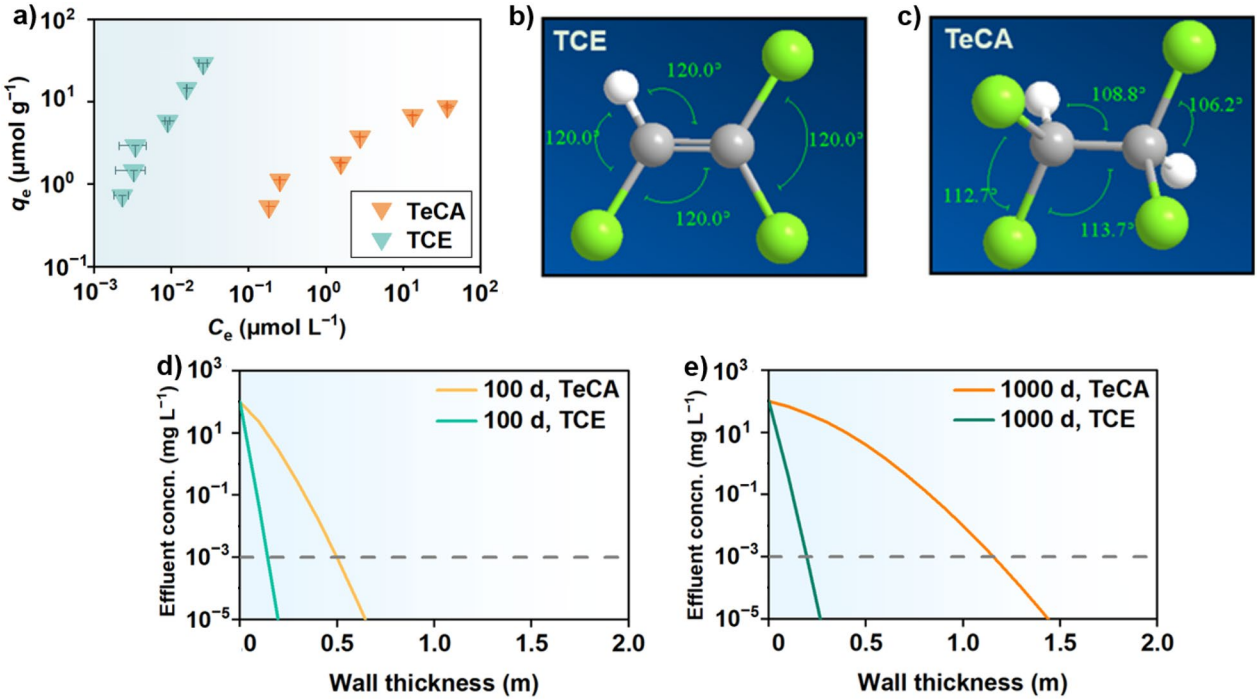

Fig. 6 Biochar-mediated transformation of TeCA significantly improves contaminant sequestration. **a** Comparison of sorption capacities of TeCA and TCE to BC600. **b**, **c** Configurations of planar TCE and nonplanar TeCA. **d**, **e** Model simulation of concentrations of TeCA and TCE in an effluent from a BC600-filled permeable reactive barrier, as affected by wall thickness from continuous constant source input at selected simulation time (100 d and 1000 d), showing that converting TeCA to the more adsorptive TCE greatly reduces the wall thickness required for contaminant sequestration

(Additional file 1: Table S1). The stronger adsorption of TCE likely was the result of the pore-filling effects, an important driving force for the adsorption of hydrophobic organic compounds to carbonaceous materials containing rigid micropores (Chen et al. 2023; Kilduff and Wigton 1999; Qiu et al. 2022). With its planar configuration (Fig. 6b), TCE molecules were prone to enter the slit pores of carbonaceous materials, as the interaction with multiple sidewalls of the micropores would result in stronger binding of the molecules (Chen et al. 2023; Xiao et al. 2018). The likelihood of entering micropores was lower for the nonplanar TeCA molecules (Fig. 6c), due to steric hindrance (Li et al. 2022; Lu et al. 2016). Similar observations have been made for nonplanar ortho-substituted polychlorinated biphenyls and planar ones with similar hydrophobicity; for example, the planar 4-chlorobiphenyl exhibited much higher extent of adsorption than the nonplanar 2,2-dichlorobiphenyl (Cornelissen et al. 2005; Pignatello et al. 2017). Moreover, the three chlorine atoms in TCE molecule have an electron induction effect that lowers the electron density in the carbon double bonds (Chen et al. 2018; Freeborn et al. 2005; Zhou et al. 2015). This would have promoted the electron donor–acceptor interactions between the electron-depleted carbon double bonds of TCE (π electron acceptors) and the electron-rich regions on the surfaces of the high-temperature biochar (π electron donors). It has been reported that π-π electron donor–acceptor interactions were a major cause for the enhanced adsorption of TCE, tetrachloroethylene and dichloroethylene to graphene materials (Zhou et al. 2015).

The implication of this enhanced binding on the remediation of chlorinated solvents-impacted groundwater is illustrated with a scenario wherein a PRB is used to intercept a TeCA plume. The effluent concentrations of contaminants can be estimated with a solute transport equation:

$$\left(1+\frac{\rho_b}{\theta}K_d\right)\frac{\partial C}{\partial t}=D\frac{\partial^2 C}{\partial x^2}-v\frac{\partial C}{\partial x}-\lambda C \quad (1)$$

where C is the effluent concentration (mg L^{-1}) of TeCA or TCE; D is the hydrodynamic dispersion coefficient (m d^{-1}); v is the seepage velocity of groundwater (m d^{-1}); ρ_b is the bulk density of the porous media (kg L^{-1}); θ is the effective porosity (dimensionless); λ is the first-order decay coefficient (d^{-1}); x is the PRB wall thickness (m) and t is the simulation time (d); and K_d (L kg^{-1}) is the adsorption coefficient of TeCA or TCE. The profiles

of effluent concentrations as a function of wall thickness clearly showed that a much thinner wall would be needed to intercept the contaminants if TeCA can be converted into TCE within the wall (Fig. 6d, e; the detailed parameters used in the solute transport equation are summarized in Additional file 1: Table S6). For instance, to keep an effuluent concentration below 0.001 mg L^{-1}, the required wall thickness needed would be 3.6–5.8 times smaller if TeCA is transformed to TCE inside the wall (two simulations, one for 100 d of PRB deployment time, and one for 1000 d are shown in Fig. 6d, e). Obviously, such increased binding capacities of biochars not only enhance the removal efficiency of contaminants, but also greatly reduce the capital and maintenance costs associated with PRB implementation.

4 Conclusions

Carbonaceous materials have shown great promise for in situ remediation of chlorinated compounds. Besides of serving as strong adsorbents, carbonaceous materials also mediate abiotic or biotic degradation. In this study, we demonstrate that biochars pyrolyzed at 600 °C and above exhibit greater efficiencies in catalyzing the dehydrochlorination reaction of TeCA than those prepared at lower temperatures (500 °C or lower). This is due to their higher contents of carbonates, the primary reactive components in catalyzing the reaction. We show that this catalytic reaction can be exploited to improve the performance of PRBs, by substantially reducing the amounts of carbonaceous fillings needed. Our work advances the understanding on the reactivity of biochars in environmental systems. Made from biomass such as stalks and wood chips, biochars are low-cost and readily available. The previously unrecognized roles of inorganic residues of biochars indicate that for the treatment of certain contaminants, biochars may even be more preferable materials than activated carbons and engineered carbonaceous nanomaterials. This advantage may be further exploited by choosing the right sources of biochar feedstocks. Moreover, to optimize the overall remediation efficiency of a contaminated site, biochars can be used in combination with other technologies, such as bioremediation and chemical oxidation/reduction technologies, as a preconditioning step that transform parent compounds to the ones that can be degraded more easily. Future studies should be carried out to understand the influences of co-existing groundwater constituents (e.g., dissolved organic matter and coexisting contaminants), to access the long-term stability, and to develop approaches to regenerating the capacity of the biochars. To ensure their sustainability in practical applications, the potential negative effects of biochars in the environment, especially the potential impact of the degradation products on the ecosystem, should also be considered.

Supplementary Information

The online version contains supplementary material available at https://doi.org/10.1007/s42773-025-00475-x.

Additional file 1: **Text S1.** Measurement of the alkaline species. **Text S2.** Adsorption of TeCA and TCE on biochars. **Table S1.** Physicochemical properties of TeCA and TCE. **Table S2.** Elemental composition of carbon and oxygen in the biochar samples. **Table S3.** Contents of alkaline species in biochar samples. **Table S4.** The fitted parameters of the reaction data in the multi-step kinetic model under varied solution conditions. **Table S5.** Freundlich model coefficients (KF and n) obtained from the adsorption isotherms of TeCA and TCE onto high-temperature biochars, using BC600 as an example. **Table S6.** Parameters of the solute transport equation. **Fig. S1.** Error distribution histograms of the multi-step kinetic model fitting for aqueous phase TeCA, solid phase TeCA, aqueous phase TCE, and solid phase TCE. **Fig. S2.** The kinetic modeling of TeCA hydrolysis occurred both in the aqueous phase and on the biochars with a multi-step kinetic model. **Fig. S3.** Effects of acid treatment on the hydrolytic ability of BC700 and BC300 for TeCA degradation. **Fig. S4.** Effects of pH on the hydrolysis of TeCA for BC700 and BC300.

Acknowledgements
The authors would like to acknowledge the China-US Center for Environmental Remediation and Sustainable Development.

Author contributions
Lin Duan: Methodology, Formal Analysis, Writing-Original Draft. Zicui Gong: Investigation, Data Curation. Yang Li: Investigation, Data Curation. Tianchi Cao: Writing-Review and Editing. Tong Zhang: Supervision, writing-Review and Editing. Wei Chen: Funding Acquisition, Conceptualization, Writing—Review and Editing. All authors read and approved the final manuscript.

Funding
This work was supported by the National Natural Science Foundation of China (22125603 and 22020102004), Tianjin Municipal Science and Technology Bureau (23 JCYBJC01650, 23 JCQNJC01340 and 21 JCJQJC00060), the Fundamental Research Funds for the Central Universities and the Ministry of Education of China (T2017002).

Data availability
All data generated or analyzed during this study are included in this published article (and its supplementary information files). The datasets generated and analyzed during the current study are available from the corresponding author on reasonable request.

Declarations

Competing interests
The authors have no competing interests to declare that are relevant to the content of this article.

Author details
[1]College of Environmental Science and Engineering, Ministry of Education Key Laboratory of Pollution Processes and Environmental Criteria, Tianjin Key Laboratory of Environmental Remediation and Pollution Control, Nankai University, 38 Tongyan Road, Tianjin 300350, China.

Received: 25 December 2024 Revised: 29 April 2025 Accepted: 11 May 2025
Published online: 10 June 2025

References

Bekele DN, Du J, De Freitas LG, Mallavarapu M, Chadalavada S, Naidu R (2019) Actively facilitated permeable reactive barrier for remediation of TCE from a low permeability aquifer: field application. J Hydrol 572:592–602. https://doi.org/10.1016/j.jhydrol.2019.03.059

Cao H, Mao J, Tratnyek PG, Xu W (2024) Role of nitrogenous functional group identity in accelerating 1,2,3-trichloropropane degradation by pyrogenic carbonaceous matter (PCM) and sulfide using PCM-like polymers. Environ Sci Technol 58:10752–10763. https://doi.org/10.1021/acs.est.3c11010

Chen B, Zhou D, Zhu L (2008) Transitional adsorption and partition of nonpolar and polar aromatic contaminants by biochars of pine needles with different pyrolytic temperatures. Environ Sci Technol 42:5137–5143. https://doi.org/10.1021/es8002684

Chen W, Li Y, Zhu D, Zheng S, Chen W (2014a) Dehydrochlorination of activated carbon-bound 1,1,2,2-tetrachloroethane: implications for carbonaceous material-based soil/sediment remediation. Carbon 78:578–588. https://doi.org/10.1016/j.carbon.2014.07.041

Chen W, Zhu D, Zheng S, Chen W (2014b) Catalytic effects of functionalized carbon nanotubes on dehydrochlorination of 1,1,2,2-tetrachloroethane. Environ Sci Technol 48:3856–3863. https://doi.org/10.1021/es405683d

Chen Z, Xiao X, Chen B, Zhu L (2015) Quantification of chemical states, dissociation constants and contents of oxygen-containing groups on the surface of biochars produced at different temperatures. Environ Sci Technol 49:309–317. https://doi.org/10.1021/es5043468

Chen M, Tong H, Li F, Liu C, Lan Q, Liu C (2018) The effect of electron donors on the dechlorination of pentachlorophenol (PCP) and prokaryotic diversity in paddy soil. Eur J Soil Biol 86:8–15. https://doi.org/10.1016/j.ejsobi.2018.01.008

Chen X, Wu B, Yang W, Zhao G, Han J, Huang C, Sun B, Wang A, Li Z (2023) Biochar as a multifunctional material facilitate the organohalide remediation: a state-of-the-art review. Chem Eng J 460:141700. https://doi.org/10.1016/j.cej.2023.141700

Chen W, Yu S, Zhang H, Wei R, Ni J, Farooq U, Qi Z (2024) Biochar-derived organic carbon promoting the dehydrochlorination of 1,1,2,2-tetrachloroethane and its molecular size effects: synergies of dipole-dipole and conjugate bases. Water Res 259:121812. https://doi.org/10.1016/j.watres.2024.121812

Cornelissen G, Haftka J, Parsons J, Gustafsson Ö (2005) Sorption to black carbon of organic compounds with varying polarity and planarity. Environ Sci Technol 39:3688–3694. https://doi.org/10.1021/es048346n

Ding K, Byrnes C, Bridge J, Grannas A, Xu W (2018) Surface-promoted hydrolysis of 2,4,6-trinitrotoluene and 2,4-dinitroanisole on pyrogenic carbonaceous matter. Chemosphere 197:603–610. https://doi.org/10.1016/j.chemosphere.2018.01.038

Ellis DE, Hadley PW (2009) Sustainable remediation white paper—integrating sustainable principles, practices, and metrics into remediation projects. Remediation 19:5–114

Fan D, Gilbert EJ, Fox T (2017) Current state of in situ subsurface remediation by activated carbon-based amendments. J Environ Manag 204:793–803. https://doi.org/10.1016/j.jenvman.2017.02.014

Fang Q, Chen B, Lin Y, Guan Y (2014) Aromatic and hydrophobic surfaces of wood-derived biochar enhance perchlorate adsorption via hydrogen bonding to oxygen-containing organic groups. Environ Sci Technol 48:279–288. https://doi.org/10.1021/es403711y

Fidel RB, Laird DA, Thompson ML (2013) Evaluation of modified Boehm titration methods for use with biochars. J Environ Qual 42:1771–1778. https://doi.org/10.2134/jeq2013.07.0285

Fidel RB, Laird DA, Thompson ML, Lawrinenko M (2017) Characterization and quantification of biochar alkalinity. Chemosphere 167:367–373. https://doi.org/10.1016/j.chemosphere.2016.09.151

Freeborn RA, West KA, Bhupathiraju VK, Chauhan S, Rahm BG, Richardson RE, Alvarez-Cohen L (2005) Phylogenetic analysis of TCE-dechlorinating consortia enriched on a variety of electron donors. Environ Sci Technol 39:8358–8368. https://doi.org/10.1021/es048003p

Hao Q, Xiao Y, Liu K, Yang H, Chen H, Wang L, Wang J, Zhang Y, Hu W, Liu Y, Li B (2025) Spatial pattern of groundwater chemistry in a typical piedmont plain of Northern China driven by natural and anthropogenic forces. Sci Rep 15(1):7643. https://doi.org/10.1038/s41598-025-91659-9

Hou D, Al-Tabbaa A, O'connor D, Hu Q, Zhu Y-G, Wang L, Kirkwood N, Ok YS, Tsang DCW, Bolan NS, Rinklebe J (2023) Sustainable remediation and redevelopment of brownfield sites. Nat Rev Earth Environ 4:271–286. https://doi.org/10.1038/s43017-023-00404-1

Hsieh H-S, Pignatello JJ (2017) Activated carbon-mediated base hydrolysis of alkyl bromides. Appl Catal B Environ 211:68–78. https://doi.org/10.1016/j.apcatb.2017.04.010

ITRC (2011) Green and sustainable remediation: state of the science and practice. Interstate Technology & Regulatory Council

Jiang M, He L, Niazi NK, Wang H, Gustave W, Vithanage M, Geng K, Shang H, Zhang X, Wang Z (2023) Nanobiochar for the remediation of contaminated soil and water: challenges and opportunities. Biochar. https://doi.org/10.1007/s42773-022-00201-x

Khalili D, Ramjerdi AA, Boostani HR, Ghaderi A (2024) Biochar: a high performance and renewable basic carbocatalyst for facilitating room temperature synthesis of 4H-benzo[h]chromene and pyranopyrazoles in water. Biochar. https://doi.org/10.1007/s42773-023-00286-y

Kilduff JE, Wigton A (1999) Sorption of TCE by humic-preloaded activated carbon: incorporating size-exclusion and pore blockage phenomena in a competitive adsorption model. Environ Sci Technol 33:250–256. https://doi.org/10.1021/es980321z

Li X, Chen W, Zhang C, Li Y, Wang F, Chen W (2016) Enhanced dehydrochlorination of 1,1,2,2-tetrachloroethane by graphene-based nanomaterials. Environ Pollut 214:341–348. https://doi.org/10.1016/j.envpol.2016.04.035

Li X, Li T, Zhang T, Gu C, Zheng S, Zhang H, Chen W (2018) Nano-TiO_2-catalyzed dehydrochlorination of 1,1,2,2-tetrachloroethane: roles of crystalline phase and exposed facets. Environ Sci Technol 52:4031–4039. https://doi.org/10.1021/acs.est.7b05479

Li Z, Jorn R, Rose V, Samonte P, Mao J, Sivey JD, Pignatello JJ, Xu W (2022) Surface-catalyzed hydrolysis by pyrogenic carbonaceous matter and model polymers: an experimental and computational study on functional group and pore characteristics. Appl Catal B-Environ 319:121877. https://doi.org/10.1016/j.apcatb.2022.121877

Li W, Zhang W, Dong J, Liang X, Sun C (2024) Groundwater chlorinated solvent plumes remediation from the past to the future: a scientometric and visualization analysis. Environ Sci Pollut Res 31:17033–17051. https://doi.org/10.1007/s11356-024-32080-z

Liang Z, Jiang C, Li Y, Liu Y, Yu J, Zhang T, Alvarez PJJ, Chen W (2024) Single-Atom iron can steer atomic hydrogen toward selective reductive dechlorination: implications for remediation of chlorinated solvents-impacted groundwater. Environ Sci Technol 58(26):11833–11842. https://doi.org/10.1021/acs.est.4c02756

Lu Z, Macfarlane JK, Gschwend PM (2016) Adsorption of organic compounds to diesel soot: frontal analysis and polyparameter linear free-energy relationship. Environ Sci Technol 50:285–293. https://doi.org/10.1021/acs.est.5b03605

Lu L, Yu W, Wang Y, Zhang K, Zhu X, Zhang Y, Wu Y, Ullah H, Xiao X, Chen B (2020) Application of biochar-based materials in environmental remediation: from multi-level structures to specific devices. Biochar 2:1–31. https://doi.org/10.1007/s42773-020-00041-7

Mackenzie K, Battke J, Koehler R, Kopinke F-D (2005) Catalytic effects of activated carbon on hydrolysis reactions of chlorinated organic compounds: part 2. 1,1,2,2-tetrachloroethane. Appl Catal B-Environ 59:171–179. https://doi.org/10.1016/j.apcatb.2005.02.005

Mauter MS, Elimelech M (2008) Environmental applications of carbon-based nanomaterials. Environ Sci Technol 42(16):5843–5859. https://doi.org/10.1021/es8006904

Moran MJ, Zogorski JS, Squillace PJ (2007) Chlorinated solvents in groundwater of the United States. Environ Sci Technol 41:74–81. https://doi.org/10.1021/es061553y

Nivorlis A, Sparrenbom C, Rossi M, Åkesson S, Dahlin T (2024) Multidisciplinary monitoring of an in-situ remediation test of chlorinated solvents. Sci Total Environ 922:170942. https://doi.org/10.1016/j.scitotenv.2024.170942

Pavlostathis SG, Jaglal K (1991) Desorptive behavior of trichloroethylene in contaminated soil. Environ Sci Technol 25(2):274–279. https://doi.org/10.1021/es00014a009

Pignatello JJ, Mitch WA, Xu W (2017) Activity and reactivity of pyrogenic carbonaceous matter toward organic compounds. Environ Sci Technol 51:8893–8908. https://doi.org/10.1021/acs.est.7b01088

Qiu M, Liu L, Ling Q, Cai Y, Yu S, Wang S, Fu D, Hu B, Wang X (2022) Biochar for the removal of contaminants from soil and water: a review. Biochar. https://doi.org/10.1007/s42773-022-00146-1

Qureshi SS, Channa A, Memon SA, Khan Q, Jamali GA, Panhwar A, Saleh TA (2021) Assessment of physicochemical characteristics in groundwater quality parameters. Environ Technol Innov 24:101877. https://doi.org/10.1016/j.eti.2021.101877
Schwarzenbach RP, Gschwend PM, Imboden DM (2017) Environmental organic chemistry. Wiley-Inter-science, New York
Seenthia NI, Bylaska EJ, Pignatello JJ, Tratnyek PG, Beal SA, Xu W (2024) Experimental and computational study of pyrogenic carbonaceous matter facilitated hydrolysis of 2,4-dinitroanisole (DNAN). Environ Sci Technol 58:9404–9415. https://doi.org/10.1021/acs.est.4c01069
Shen Y, Fang Q, Chen B (2015) Environmental applications of three-dimensional graphene-based macrostructures: adsorption, transformation, and detection. Environ Sci Technol 49:67–84. https://doi.org/10.1021/es504421y
Simon JA (2015) Editor's perspective—an in situ revelation: first retard migration, then treat. Remediation 25:1–7. https://doi.org/10.1002/rem.21420
Sizmur T, Fresno T, Akgül G, Frost H, Moreno-Jiménez E (2017) Biochar modification to enhance sorption of inorganics from water. Bioresour Technol 246:34–47. https://doi.org/10.1016/j.biortech.2017.07.082
Stratford JP, Hutchings TR, FaaM DL (2014) Intrinsic activation: the relationship between biomass inorganic content and porosity formation during pyrolysis. Bioresour Technol 159:104–111. https://doi.org/10.1016/j.biortech.2014.02.064
Stroo HF, Ward CH (2010) In situ remediation of chlorinated solvent plumes. Springer, New York
Twagirayezu G, Cheng H, Wu Y, Lu H, Huang S, Fang X, Irumva O (2024) Insights into the influences of biochar on the fate and transport of pesticides in the soil environment: a critical review. Biochar. https://doi.org/10.1007/s42773-024-00301-w
USEPA (2008) Green remediation: incorporating sustainable environmental practices into remediation of contaminated sites
Wilkin RT, Lee TR, Sexton MR, Acree SD, Puls RW, Blowes DW, Kalinowski C, Tilton JM, Woods LL (2019) Geochemical and isotope study of trichloroethene degradation in a zero-valent iron permeable reactive barrier: a twenty-two-year performance evaluation. Environ Sci Technol 53(1):296–306. https://doi.org/10.1021/acs.est.8b04081
Xiao X, Chen B, Chen Z, Zhu L, Schnoor JL (2018) Insight into multiple and multilevel structures of biochars and their potential environmental applications: a critical review. Environ Sci Technol 52:5027–5047. https://doi.org/10.1021/acs.est.7b06487
Xiao X, Chen Z, Chen B (2020) Proton uptake behaviors of organic and inorganic matters in biochars prepared under different pyrolytic temperatures. Sci Total Environ 746:140853. https://doi.org/10.1016/j.scitotenv.2020.140853
Xie Q, Yang X, Sarkar B, Dou X, Withana PA, Ok YS (2023) Conversion of biochar into sulfonate-bearing solid acids used for the hydrolysis of tylosin: the effect of aromaticity and degree of condensation. Biochar. https://doi.org/10.1007/s42773-023-00277-z
Xu X, Zhao Y, Sima J, Zhao L, Mašek O, Cao X (2017) Indispensable role of biochar-inherent mineral constituents in its environmental applications: a review. Bioresour Technol 241:887–899. https://doi.org/10.1016/j.biortech.2017.06.023
Xu W, Segall ML, Li Z (2020) Reactivity of pyrogenic carbonaceous matter (PCM) in mediating environmental reactions: Current knowledge and future trends. Front Environ Sci 14:86. https://doi.org/10.1007/s11783-020-1265-6
Yang J, Pan B, Li H, Liao S, Zhang D, Wu M, Xing B (2016) Degradation of p-nitrophenol on biochars: role of persistent free radicals. Environ Sci Technol 50:694–700. https://doi.org/10.1021/acs.est.5b04042
Yang B, Dai J, Zhao Y, Wu J, Ji C, Zhang Y (2022) Advances in preparation, application in contaminant removal, and environmental risks of biochar-based catalysts: a review. Biochar. https://doi.org/10.1007/s42773-022-00169-8
Yuan J, Xu R, Zhang H (2011) The forms of alkalis in the biochar produced from crop residues at different temperatures. Bioresour Technol 102:3488–3497. https://doi.org/10.1016/j.biortech.2010.11.018
Yuan Y, Bolan N, Prévoteau A, Vithanage M, Biswas JK, Ok YS, Wang H (2017) Applications of biochar in redox-mediated reactions. Bioresour Technol 246:271–281. https://doi.org/10.1016/j.biortech.2017.06.154
Zhang S, Mao G, Crittenden J, Liu X, Du H (2017) Groundwater remediation from the past to the future: a bibliometric analysis. Water Res 119:114–125. https://doi.org/10.1016/j.watres.2017.01.029
Zhou Y, Apul OG, Karanfil T (2015) Adsorption of halogenated aliphatic contaminants by graphene nanomaterials. Water Res 79:57–67. https://doi.org/10.1016/j.watres.2015.04.017
Zhu H, Liu X, Jiang Y, Lin D, Yang K (2022) Sorption kinetics of 1,3,5-trinitrobenzene to biochars produced at various temperatures. Biochar. https://doi.org/10.1007/s42773-022-00157-y